Crystallography, Biochemistry and Genetics of Halophilic and Thermophilic Ribosomes

I. Agmon*, H. Bartels°, A. Bashan*, W.S. Bennett°, Z. Berkovitch-Yellin*°, N. Böddeker#, A. Dribin*, M. Eisenstein*, F. Franceschi#, H.A.S. Hansen°, J. Harms°, W. Jahn+, S. Krumbholz°, I. Levin*, M. Malemud*, S. Morlang#, M. Peretz*, I. Sagi*#, F. Schlünzen°, R. Sharon*, J. Thygesen°, N. Volkmann°, V. Weinrich*, S. Weinstein* and A. Yonath*°

**Department Structural Biology, Weizmann Institute of Science, Rehovot, Israel; °Max-Planck-Laboratory for Ribosomal Structure, Hamburg, Germany; #Max-Planck-Institute for Molecular Genetics, Berlin, Germany; +Max-Planck-Institute for Medical Research, Heidelberg, Germany*

Abstract

Crystals of ribosomal particles, diffracting best to 2.9 Å resolution are being grown. Crystallographic data are being collected from shock frozen crystals with intense synchrotron radiation at cryo temperature. For obtaining phase information, heavy atom derivatives were prepared either by soaking in solutions of multi-metal salts or by specific and quantitative binding of a monofunctional reagent of an undecagold cluster. Data collected from both systems yielded interpretable difference Patterson maps. The gold cluster derivatized particles led to the first low-resolution electron density map of ribosomal particles, phased solely by experimental methods.

To create potential binding sites for heavy atom clusters on the halophilic and ribosomal particles, from which the crystals diffracting to the highest resolution are grown, exposed sulfhydryls are being inserted by site directed mutagenesis. For choosing appropriate locations for these insertions, the surface of the ribosome is being mapped by labeling naturally exposed amino and sulfhydryl groups.

An internal complex of rRNA and r-protein was isolated from the halophilic ribosome. Chimeric complexes were reconstituted with the components of this complex and the corresponding *E. coli* ones, indicating a rather high homology despite the evolution distance.

Models of the ribosome and its large subunit were reconstructed, respectively, from electron micrographs of tilt series of their monolayers, at 47 and

30 Å resolution. The similarities between these models enabled assessment of their reliability and led to tentative assignments of several functional features, including the presumed sites for binding mRNA, for the codon-anticodon interactions and for the sheltered path taken by nascent protein chains. They also hinted at possible modes of tRNA binding. The reconstructed images are being used for initial phasing of the X-ray diffraction data at low resolution. They also stimulated the design and the crystallization of complexes mimicking defined functional states, of a higher quality than that found for isolated ribosomes.

Introduction

The translation of the genetic code into polypeptide chains is a fundamental cellular process. In rapidly growing bacterial cells the biosynthetic machinery constitutes about half of the dry weight of the cell, and the biosynthetic process consumes up to 80% of the *cell's energy (1). The process of protein biosynthesis is mediated in all living cells by an organelle called the ribosome, which is a highly complicated ribonucleoprotein particle, operating as a giant multi-functional enzyme with a large range of tasks and constraints. The ribosome is built of two structurally independent subunits of unequal size, which associate upon initiation of protein biosynthesis. A typical bacterial ribosome contains about a quarter of a million atoms and is of a molecular weight of approximately 2.3 million daltons. About one third of its mass comprises of some 58–73 different proteins, depending of the source. The rest is ribosomal RNA (total of about 4500 nucleotides), which was shown to actively participate in the biosynthetic process (2–3).

Results of intensive biochemical, biophysical and genetic studies illuminated several functional aspects of the translational apparatus and led to suggestions for the overall shape and the quaternary structure of the ribosome, for the spatial proximities of various ribosomal components, for the secondary structure of a part of the ribosomal RNA chains and for the approximate position of some reaction sites. However, the understanding of the molecular mechanism of protein biosynthesis is still hampered by the lack of molecular models. For this aim three-dimensional crystals of ribosomes, their functional complexes and their subunits, diffracting best to 2.9 Å resolution, have been grown (Table I) and are being investigated by X-ray and neutron crystallography using synchrotron radiation (4–8).

So far all crystals of ribosomal particles were grown from biologically active particles. Furthermore, it was found that chemically treated particles crystallize only if the preparations used for the modifications were originally homogeneous and highly active. It is noteworthy that the integrity and the functional activity of the crystalline ribosomal particles are maintained for extremely long

periods, despite the *in-vivo* and *in-vitro* natural instability of ribosomes and their tendency to disintegrate even under favorable conditions. Aiming at elucidating the structure of the ribosomal particles at conformations closest to those required for their activity, special procedures were designed for data collection from crystals immersed in solutions mimicking the physiological environment within the cells.

It was found that the quality of the ribosomal crystals is related to the level of extremeness of the natural environment of the bacterium (Table I). Thus, the best crystals are of ribosomes from extreme halophiles, and those from extreme thermophiles yield better crystals than the moderate ones, presumably because of their higher stability. The Dead Sea contains the highest salt concentrations of any natural bodies of water in the world. Despite this extreme salinity, it supports the growth of several species of micro-organisms, all of which exhibit the unusual property of withstanding high salt concentrations and elevated temperatures. One of these organisms is the archaebacterium *Haloarcula marismortui*. The ribosomes of this bacterium function at 3.5–4 M monovalent salinity at up to 60 °C, conditions which usually cause the dissociation of nucleoprotein assemblies and the denaturation of isolated proteins. The ribosomal crystals diffracting to the highest resolution (2.9 Å) are of the large subunits of ribosomes from this bacterium (4).

Source	Grown form	Cell dimensions (Å)	Resulution (Å)
T70S	MPD*	524 x 524 x 306; $P4_12_12$	app..20
T70S (complex)#	MPD	524 x 524 x 306; $P4_12_12$	12
T30S	MPD	407 x 407 x 170; $P42_12$	7.3
H50S**	PEG*	210 x 300 x 565; $C222_1$	2.9
T50S	AS*	459 x 495 x 196; $P4_12_12$	8.7
B50S^	A*	360 x 680 x 920; $P2_12_12$	app. 18
B50S^**	PEG	308 x 562 x 395; 114°; C2	11

Table I. Characterrized three-dimensional crystals of ribosomal particles.

Crystallographic studies

The weak diffraction power of the ribosomal crystals and their large unit cell dimensions dictate the performance of virtually all the crystallographic studies with synchrotron radiation of a high brightness. At ambient temperature the higher resolution diffraction of all ribosomal crystals decays within the first instances of irradiation. Assuming that the decay is caused by propagating free radicals, formed by the X-ray beam, we developed special procedures for eliminating the movement of these radicals within the irradiated crystals, by lowering the temperatures to cryogenic limits. Special protocols were designed for the precooling and shock-freezing steps (Table II) which accommodate the unique problematic features of the ribosomal crystals: fragility, sensitivity and extremely thin edges (7,9).

Cristal form	Grown from	Freezing solution	Soaking	
T70S T30S	12% MPD*	30% MPD	15 min	months
B50S	2% PEG* (6K)	10% EG* 10–20% PEG (10–20K)	6hrs	20hrs
T50S	1.5 M AS* 2 M AS	10–15% EG	30 min	40 hrs
H50S	1.8 M KCl 0.5 M NH4Cl 0.1 M $MgCl_2$ 1–2 mM Cd^{++} 6–7% PEG (6K)	18% EG 3 M KCl 0.5 M NH4 Cl 0.1 M $MgCl_2$ 1–2 mM Cd^{++} 10% PEG (6K)	15 min Gradual addition From: 8% EG To: 18% EG	30 min

Table II. Pre-freezing treatment

It was found that properly shock-frozen crystals diffract at 90–100 K with no observable decay for periods sufficient for the collection of more than a full data-set from an individual crystal. In general, the shock frozen crystals exhibit the average mosaic spread as those exposed at ambient temperatures, and in some cases they yield data of higher resolution than those measured at ambient temperatures, as the frozen ones can be exposed longer. Furthermore, the irradiated crystals can be stored for months at cryo-temperatures and still maintain their diffracting power.

The shock frozen crystals yield crystallographic data of reasonable quality, which in many cases are of quality comparable to those obtained from crystalline proteins of average size. Thus, for above 70% completeness, the typical values for R-merge(I) at 3.5–6 Å resolution are in the range of 4–12% for the crystals of the large ribosomal subunits of *H. marismortui* (Hansen, Berkovitch-Yellin and Bashan, to be published). As mentioned above, these crystals diffract to 2.9 Å, the highest resolution obtained so far from crystals of ribosomal particles (Figure 1). They are of reasonable mosaicity (0.2–0.6°) and adequate mechanical stability. They reach an average size of 0.3 x 0.3 x 0.01 mm, have cell dimensions of 210 x 300 x 565 Å and $C222_1$ symmetry (4).

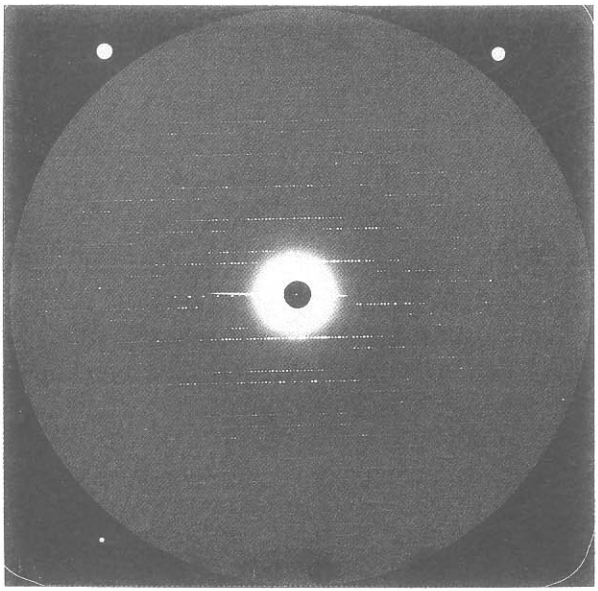

Figure 1. A rotation photograph of a crystal of H50S, obtained at 90 K at Station F1/CHESS, operating at 5.3 Gev and 50 mA. Crystal to film distance = 220 mm, collimator = 0.1 mm; wave length = 0.9091 Å.

An interantive-parallel phasing strategy

Assignment of phases to the observed structure factor amplitude is a crucial step for the construction of electron-density maps. Since the phases cannot be directly measured, their elucidation remains the less predictable and the most difficult task in structure determination of biological macromolecules. Clearly, for ribosomal crystals, the magnitude and the complexity of this step require special algorithm. Consequently, an iterative-parallel strategy has been developed,

which takes advantage of fashionable alongside with somewhat outdated procedures (Table III).

Very low resolution
• Determination the packing motifs from the diffraction of thin sections of embedded crystals investigated by EM
• Real space searches using the reconstructed models
• Reciprocal space searches (exploiting crystal symmetry)
• Solvent contrast, including anomalus for the determination of the particle's envelop, also with neutrons
• Computational methods: ab initio, such as maximum entropy
Medium resolution
• MIR, SIR, MAD: the use of monofunctional reagents of dense multi heavy-atom clusters (undecagold and tetrairidium) for direct, specific and quantitative pre-crystallization binding
• Crystallization of core particles, lacking specific proteins
• Specific modifications (with heavy atom clusters) of nucleic acids which bind to ribosome: tRNA, mRNA and cDNA
High resolution
• Soaking crystals in multi-metal salt solutions
• Specific binding of a tetrairidium cluster to a few sites
• Phase extension
• Molecular replacement, using high resolution structures of isolated nucleoprotein complexes

Table III. An interative-parallel phasing strategy.

Phasing at low resolution

Although phasing at low resolution is rarely used in protein crystallography, there have been sufficient indications to stimulate such efforts as initial and intermediate steps in phasing the diffraction data collected from the ribosomal crystals. The Maximum Entropy method, combined with Likelihood Gain for phase-set discrimination (11–12) have already led to initial phasing at 60 Å resolution. Furthermore, the resulting packing arrangement coincides with the those obtained by DM and MR (Berkovitch-Yellin, Eisenstein, Bashan, Pebay-Peyroula Roth and Schlünzen, to be published) and by global minimum determined by an R-factor searches using spherical Gaussians to represent the particles (Volkmann et al., to be published).

Direct information about packing motifs of the ribosomal crystals is being derived by electron microscopy. Three-dimensional crystals are embedded in epon, and sectioned at preferred orientations to extremely thin slices, of a width similar to that of a single unit cell. Optical diffraction information, obtained from their electron-micrographs, combined with visual inspection and symmetry considerations, are then used for the determination of the packing motifs of the crystals (Agmon et al., to be published). The resulting arrangements are tested visually and by conventional crystallographic methods, exploiting comparisons of calculated and observed structure factors. Experimental procedures are being combined with the computational methods. One of them is the Solvent Contrast Variation (13) and its extension, using anomalous signals (MASC, multi wavelength solvent contrast). This method is based on extracting the envelop of the particle from structure factors free of the contribution of the intra-crystal solvent, using crystals immersed in solutions containing high amounts (0.3–1.5 M) of compounds of varying electron densities (Table IV). As variations of the solvent diffraction are being exploited, data were collected to the resolution limits mostly influenced by the solvent (>12 Å). The favorable compound for soaking is goldthioglucose (Schlünzen et al., to be published).

High concentration, 0.2–1.5 , of:
1. GTG (gold thio glucose), for crystas grown from MPD or ammonium sulfate
2. ammonium selenate, for crystals grown in ammonium sulfate, for crystals grown in ammonium sulfate
3. CsCl, RbCl, KBr, RbBr, LiCl, for crystals grown at high salt (halophilic bacteria)

Table IV. Materials used for soaking for solvent contrast variation

It is suitable for all crystal forms except for H50S, which are stabilized in solutions containing higher than 3.5 M salts. For these crystals the main constituent in the stabilization solution (Kcl) are being gradually exchanged by compounds of a similar chemical nature, albeit different electron densities. The solvent contrast method is also the basis for experiments with neutron crystallography (14).

The approximate models reconstructed for the ribosome and its large subunit from *B. stearothermophilus* (15–16 and Figure 2), are being employed in rotation and translation search methods. The use of reconstructed images of ribosomal particles of one bacterium with crystallographic data obtained from crystals of

tals of ribosomes from another one is based on the assumption that at the resolution limits (28–47 Å) of the reconstructions the gross structural features of prokaryotic ribosomes are rather similar.

Attempts at phasing by "traditional" MIR experiments (soaking)

In bio-macromolecular crystallography the commonly used methods for phasing are MIR and SIR, both require a quantitative attachment of heavy atoms at a limited number of sites within the unit cell and a reasonable isomorphism between the native and the derivatized crystals. The differences in the intensities of the reflections of the native and derivatized crystals are being exploited for phase determination, therefore the added compounds are chosen according to their potential ability to induce measurable signals.

Heavy-atom derivatives of crystals of biological macromolecules are routinely obtained by soaking crystals in solutions of the heavy-atom compounds or by co-crystallization of the macromolecule together with the heavy atom. Using these procedures, productive single-site derivatization is largely a matter of chance, but the chances of obtaining a useful derivative for a typical macromolecule are sufficiently high that more sophisticated techniques are rarely needed. For proteins of average size (e.g. with molecular weights of 15–80K daltons), useful heavy atom derivatives consist of one or two heavy-metal atoms. Because of the large size of the ribosome, ideal compounds for derivatization are compact and dense materials of a proportionally larger number of heavy-atoms.

For medium resolution phasing, two clusters are being used, comprised of densly packed heavy metal atoms: an undecagold cluster, with a total molecular weight of 6,200 daltons and a tetrairidium cluster, of a molecular weight of 2,300 daltons (Figure 3 and see refs. 8,17–20). Although both clusters have been known for quite some time, they were never used for phasing. As the core of the undecagold cluster is about 8.2 Å in diameter (17), it can be treated as a single scattering group at low to medium resolution. The tetrairidium cluster has a core diameter smaller than 5 Å (18), thus it can be treated as a "single heavy atom" at somewhat higher resolution. Both clusters are of a very high electron density, consisting of cores in which the metal atoms are linked directly to each other. These cores are embedded within a dense chemical sphere, designed to increase the solubility and the stability of the clusters. Therefore these clusters cannot be used for soaking, but have been designed for direct binding, as described below (in Specific labeling).

Anticipating high resolution structure, multi-atom salts are being used for soaking experiments, similar to those traditionally performed for average size proteins, despite the high risk of multiple-site attachment.

In typical experiments, crystals of H50S, T50S and T30S are being soaked for 1–30 days in solutions of mM concentrations of salts of multi W atoms (Table V), which, according to simulation studies, should have measurable signals (Volkmann and Thygesen, to be published). Although so far the resolution of the soaked crystals is somewhat lower than that of the native ones, preliminary studies showed that in several cases the soaking did not harm the crystal's network and did not induce significant nonisomorphism. Furthermore, for the case of the $K_{14}NaP_{14}W_{110}O_{110}$ salt, the resulting interpretable difference Patterson maps indicated clearly the phasing power of this salt (Hansen et al., to be published).

TAMM = tetrakis (acetoxymercuri-metane)
$(NH_4)_6\,(P_2W_{18}O_{62})\ 14\,H_2O$
$(NH_4)_6\,(P_2W_{17}CoO_{62})\ 14\,H_2O$
$K_{14}NaP_5W_{30}O_{110}$
$(K_5O_2)_3(PW_{12}O_{40})$
$Na_{16}((O_3PCH_2PO_3)_4W_{12}O_{36})\ nH_2O$
Ta_6Cl_{14}
$Ta_6Br_{12}\ 2H_20$
Nb_6Cl_{14}

Table V. Multi-metal salts, for MIR phasing.

Reasonable isomorphism is a prerequisite for MIR-type phasing. For ribosomal crystals, in some instances, striking isomorphism was observed. In others, apparent heterogeneity was detected even among individual crystals grown and examined under the same conditions. To remove doubts concerning the influence of the shock-freezing on isomorphism, the reproducibility of the freezing procedure has been assessed. To address the hypothesis that the inherent flexibility of the ribosome allows variability in the shrinkage of the unit cell vectors upon freezing, crystals were cut and each of their parts was frozen and measured separately. The observed negligible differences in cell dimensions (0.25%) manifested the high reproducibility of the shock cooling process (Table VI and ref. 21). These findings are most important for future phasing experiments as they demonstrate that the isomorphism is maintained, despite the mechanical and chemical stresses involved in the process of shock freezing.

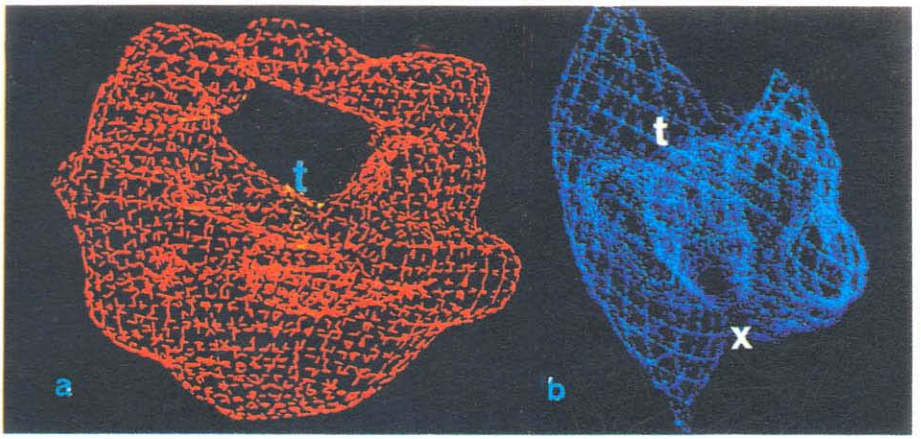

Figure 2. A computer graphics display of the outer contours of the models, reconstructed from negatively stained crystalline arrays of (a) 70S ribosomes from *B. stearothermophilus* at 47 Å resolution (16) and (b) 50S subunit from the same bacteria (15). t points at the entrance to three internal tunnels and X shows the exit from it.

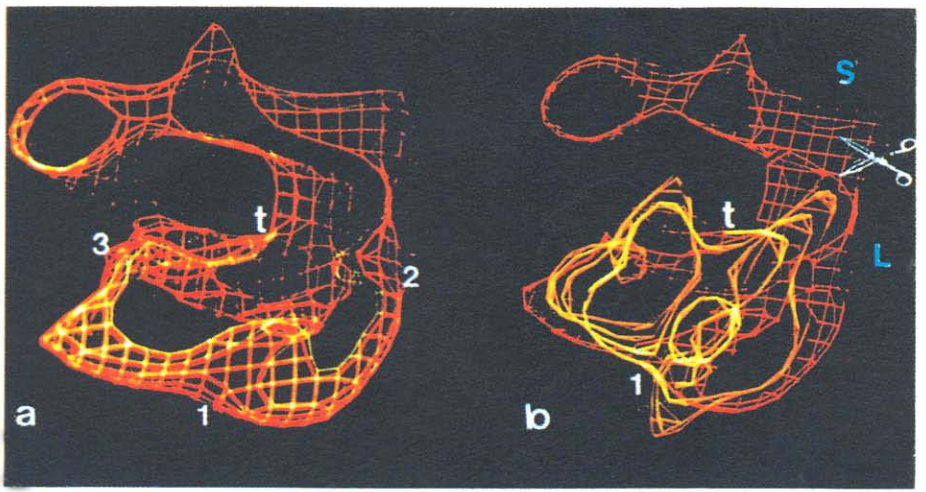

Figure 4. A slice of about 50 Å in thickness, through the model of the 70S ribosomes. t points at the common entrance to the three internal tunnels, and the numbers 1, 2 and 3 show the exits sites from tunnels t1, t2 and t3 respectively. (b) is a superpositions of comparable slices of the reconstructed model of the 50S subunit, on the sliced 70S ribosome (in orange) aligned so that its main tunnel coincides with tunnel t1. The scissors point at the assumed contact region between the 30S (S) and the 50S (L) subunits.

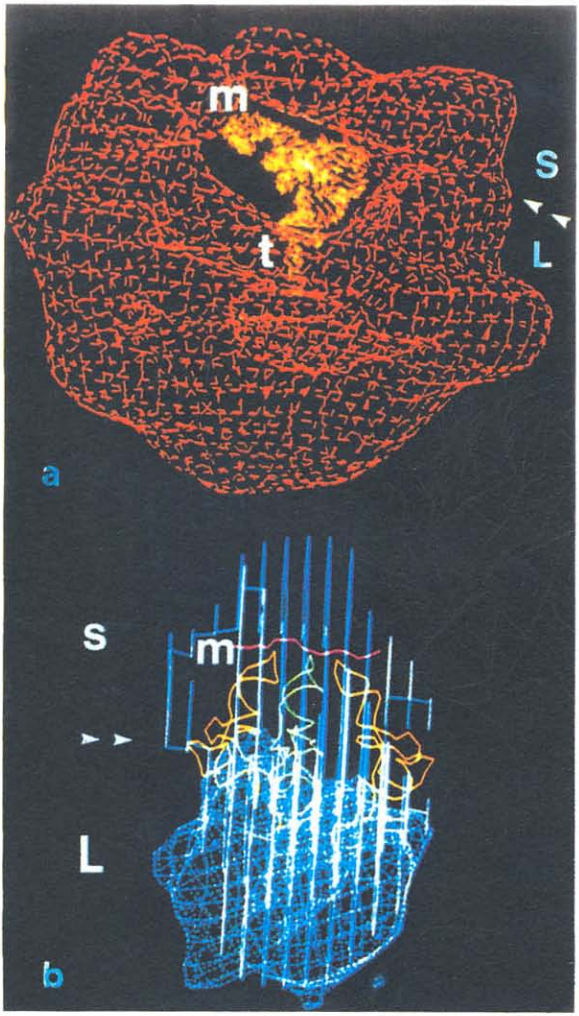

Figure 5. (a) The current interpretation of the ribosomal features. The arrow heads show the approximate directions of the interface between the S (small = 30S) and L (large = 50S) subunits. t points at the entrance to the tunnel. The presumed positions of the bound part of the mRNA chain are marked by m. A model built tRNA is shown in the two reconstructed models of the ribosome. (b) A perpendicular view of the ribosome (contours shown in light blue lines), showing that the free space at the intersubunit interface is large enough to accommodate three binding sites for tRNA molecules, two with their CCA end very close to the entrance of the tunnel, and the third, somewhat further away, presumably in a position allowing less tight contacts (the left tRNA molecule in this figure). Our aim was to show the availability of space for three sites, not to suggest that three tRNA molecules are bound to the ribosomes simultaneously. The 50S subunit is highlighted as a blue net.

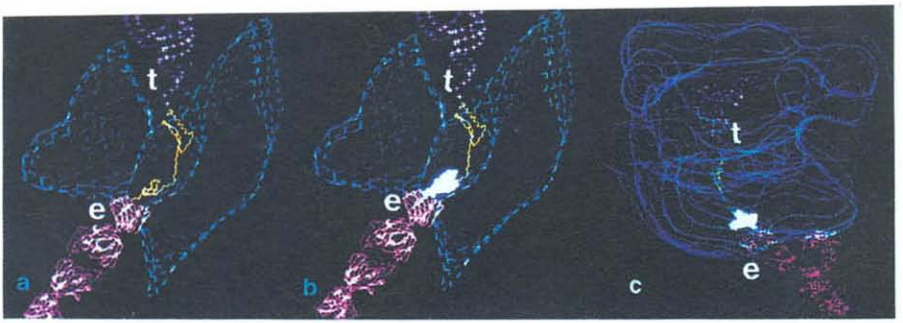

Figure 6. (a) A slice of 50 Å thickness of the 50S subunit (in blue), into which the main chain of the MS2 coat protein was modeled. The protein was placed along the tunnel in a partially unfolded conformation, maintaining the native fold of its beta-stretches and the native (crystallographically determined) conformation of the segment 1–47. The C-terminus was placed in the vicinity of the proposed peptidyl transferase center and the N-terminus at the exit domain of the tunnel. A molecule of IgG, recognizing a probe attached to the N-terminal was positioned at the end of the tunnel (69,72). t shows the entrance to the tunnel and e, its exit. (b) As (a), but the region 1–47 includes all atoms and shown as a space-filling structure. (c) As (b), but the whole 70S ribosome is shown.

	H50S collected at F1/CHESS (FUJI IP)	**H50S** collected at X11/EMBL (MAR)	**T50S** collected at X11/EMBL (FUJI IP)
Part I	211.0 300.0 563.5	212.0 301.7 567.9	493.1 493.1 197.8
Part II	211.0 300.0 563.0	212.2 301.8 567.7	492.7 492.7 197.7

Table VI. Cell dimensions of cut crystals

Specific labeling of 50S ribosomal subunits by the undecagold cluster led to phasing

Since ribosomal particles have an extremely large and complex surface area, it is preferable to specify the nature and control the extent of the binding of the heavy atom prior to the crystallization. Thus, the alternative procedure for derivatization is covalent binding of the heavy atom compound to the molecule at one or a few specific sites before crystallization. This approach requires sophisticated synthetic techniques and time-consuming purification procedures, but it offers a much better chance of obtaining unique derivatives. Specific derivatization of selected ribosomal components may have a considerable value not only in phasing the crystallographic data, but also in localization of their sites on the ribosomes, information which may be indispensable for the interpretation of the maps.

Assuming reasonable isomorphism and a full single-site occupancy of the undecagold cluster, the average differences in diffraction intensities between native and gold-cluster bound ribosomal particles are expected to be about 19%, 15% and 11% for the 30S, 50S and 70S particles, respectively (19). Hence, provided these requirements are fulfilled, the undecagold-cluster is likely to induce measurable differences between the intensities of the reflections of the native crystals and those of the derivatized ones. Simulation studies confirmed the above calculations and indicated adequate phasing power (Volkmann and Bartels, to be published).

A procedure was designed for the derivatization of the ribosomal crystals (19–20). For assessing its suitability, we took advantage of the knowledge of the biochemistry and genetics of the 50S ribosomal subunits from *Bacillus stearothermophilus*, although the crystals of these particles diffract very weakly to rather limited resolution (Table I). A mutant, lacking one ribosomal protein, BL11, was obtained by the addition of the antibiotics thiostrepton to the bacterial growth medium (22). In parallel, protein BL11 was isolated from native particles (23). It was found that the cores lacking protein BL11 crystallize almost isomorphousely with the native ones, indicating that the removal of this protein caused neither major conformation changes in the ribosome, nor disturbances in the crystal's network.

To facilitate quantitative and site specific derivatization, a monofunctional reagent was synthesized from the undecagold cluster (20). To enable the binding of the clusters, their accessibility was increased by attaching a short and rather rigid chemically reactive arm. The first targets for binding the clusters were exposed free sulfhydryls. Therefore, the monofunctional arm had either a maleimido or an iodoacetyl moiety at its end (Figure 3). The latter was designed to avoid the chirality which may be introduced by the reaction of the -SH with

the double bond of the maleimido moiety (8). The monofunctional undecagold cluster was bound quantitatively to the isolated ribosomal protein, BL11, exploiting its only exposed cysteine. The modified protein was, in turn, reconstituted into cores of mutated ribosomes lacking it, although the binding of the cluster was carried out under mild denaturing conditions. The crystals of the so obtained fully derivatized B50S particles yielded data of reasonable quality, and the resulting SIR 20 Å resolution electron-density map is of reasonable quality and contains features of a size similar to that observed for large ribosomal subunits by electron microscopy (Bartels et al., to be published).

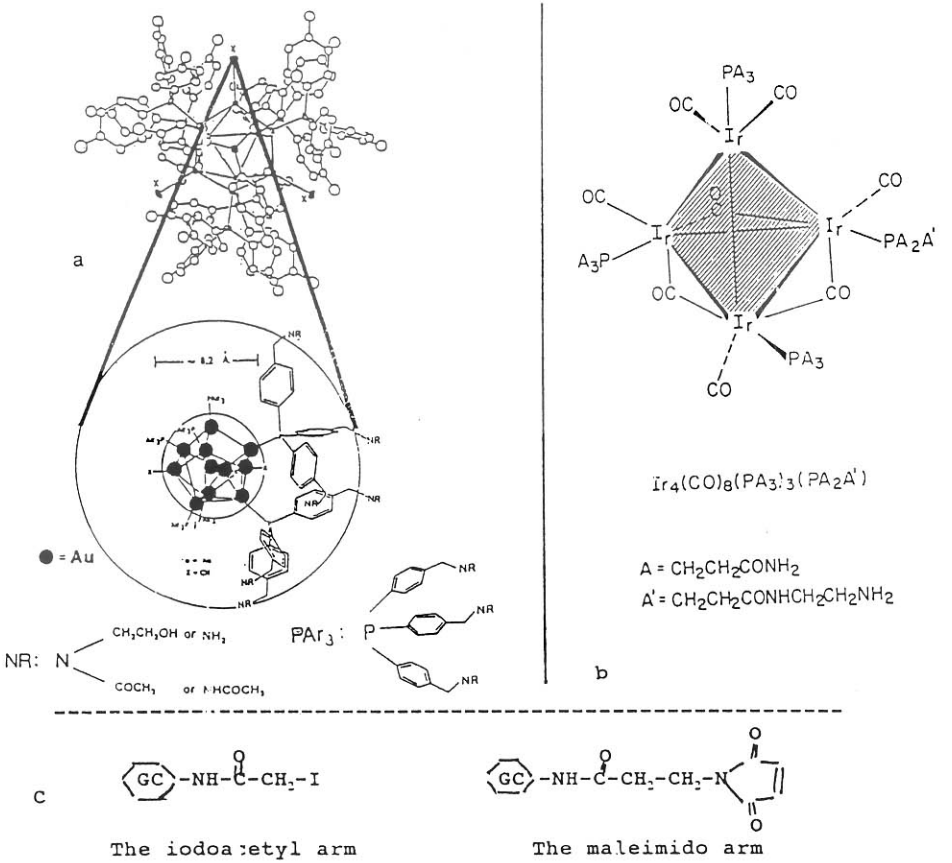

Figure 3. Schematic representations of (a) the undecagold, (b) the tetrairidium clusters and (c) their monofunctional handles.

The extension of eubacterial biochemistry to the halophilic and the thermophilic systems

The suitability of the undecagold cluster for phasing data collected from crystals of the 50S subunits from *B. stearothermophilus*, encouraged extension of this procedure to the ribosomal particles from *H. marismortui* and *Thermus thermophilus*, which yield crystals of a much higher quality. However, this task was hampered by severe difficulties. Because of the significant resistance of the halophilic ribosomes to mutagenesis (24) no protein-depleted core particles could be produced by growing the bacteria on medium containing antibiotics. Also, the chemical methods used for quantitative splitting of the *E. coli* ribosomal proteins were found unsuitable for the halophilic and thermophilic systems. Furthermore, in contrast to the ease of the incorporation of the gold-cluster bound protein BL11 into depleted cores of *B. stearothermophilus*, protein HmaL11, the presumed halophilic homolog of BL11, can be reconstituted into core H50S particles only when its sulfhydryl group is free. Therefore, as is, it is not useful for derivatization. Consequently, the potential heavy-atom binding sites on the surfaces of the halophilic and thermophilic ribosomes are being inserted by chemical or genetic procedures (25–26). As the genes of most of the halophilic and thermophilic proteins have been cloned (27), the insertion of chemically reactive functional groups onto the surface of the ribosome became feasible (26). The choice of the appropriate locations for these insertions is based on the advanced stage of the sequencing of the halophilic r-proteins (28) and on surface mapping experiments, performed either by limited proteolysis (29) or by direct chemical determination of exposed amino and sulfhydryl groups. Procedures have been developed for selective detachment of ribosomal proteins (Table VII).

Bacillus stearothermophilus 50S lacking protein BL11 (obtained by mutagenesis)
Haloarcula marismortui 50S lacking HmaL11 (obtained by chemical methods)
Haloarcula marismortui 50S lacking HmaL11, HmaL12, HmaL6 (obtained by chemical methods)
Thermus thermophilus 30S with modified S8 (obtained by mutagenesis)
Thermus thermophilus 70S with modified S8 (obtained by mutagenesis)

Table VII. Crystallization of core particles lacking ribosomal proteins

Four ribosomal proteins were removed quantitatively by dioxane from the large halophilic subunit (H50S) and two from the small one (H30S), all of which could be fully reconstituted into the depleted core particles. As mentioned above, one of these split proteins, HmaL11, binds reagents specific to -SH groups, but the derivatized protein could not be incorporated into the core particles. However, using this property, cores of H50S subunits depleted of one protein (HmaL11) were obtained. The relative ease of the detachment of HmaL11 from the halophilic, as well as the homologous protein from various bacterial ribosomes, poses the interesting question as to the role of this protein in the translational process. Clearly, this protein is not absolutely necessary for protein biosynthesis and its in situ interactions are rather weak. Similar to the case of BL11, the ribosomal subunits lacking protein HmaL11 crystallize under the same conditions as native H50S and show apparent isomorphism with them, suggesting that the depletion of this protein does not cause major conformational changes, and that it is not involved in the crystal's network.

The problematic nature of the ribosomal surface

An exact definition of the surface of the halophilic ribosomes is hampered by the still not identified parameters influencing the compactness of the ribosomes. Even the surface of the *E. coli* ribosome, which is considered to be the best characterized one, is still not totally known, mainly because of its significant inherent conformational heterogeneity. Thus, it has been recently suggested that almost all properties assigned to the *E. coli* ribosome were actually identified only for subsets of ribosomal populations, and may not reflect the overall behavior (30).

Although almost three decades ago it was suggested by Sir F. Crick that the original ribosome was made entirely of RNA, until recently it was assumed that the catalytic activities of the ribosome are carried out solely by the ribosomal proteins and the ribosomal RNA has more passive roles, such as providing the scaffold for the ribosomal network. Besides the general tendency to assign enzymatic activities to proteins rather than to RNA molecules, there were sound reasons for these assumptions. Thus, traditional electron microscopy as well as low-resolution contrast methods (mainly light and neutron scattering) were initially over-interpreted as if the ribosomal core consists mainly of rRNA, and that this core is covered by the ribosomal proteins. Biochemical experiments challenging the above dogma have been recently designed. These were stimulated by the demonstrations of the catalytic nature of RNA in several biological systems, as well as by evidence concerning the nature of the ribosomal RNA. Thus, volume considerations and crosslinking data suggest an intervening rRNA-protein arrangement, with only a few proteins located close to the

surface. Moreover, affinity labeling experiments, the substantial conservation in some rRNA regions, the possibility of blocking of several crucial ribosomal activities by hybridization with anti-sense DNA or by antibiotics which are known to cleave rRNA, indicate that a significant amount of rRNA is exposed as single stranded. Consequently, the ribosomal functions are no longer attributed solely to the ribosomal proteins, and several distinct ribosomal functions have been attributed, at least partially, to the rRNA (30). Furthermore, some of the difficulties in the crystallization of the ribosomal particles may result from the exposure of the rRNA.

---

a. Bacillus stearothemophilus
Complimenting the region of 23S rRNA (50S), which is masked by protein BL11 in native particle, but becomes exposed in a mutant, lacking this protein (grow on thiostrepton). Bases: 1125–1158

b. Thermus thermophilus
Complimenting the vicinity of "Shine Dalgarno" region on 16S rRNA (30S): the last 14 from the 3' end
Complimenting the " alpha sarcin" binding site on 23S RNA (50S). Bases: 2646–2667 (E. coli's equivalents)

c. Haloarcua marismortui
Complimenting the region of 23S rRNA (50S) which binds thiostrepton in E. coli. Bases: 1422–1432
Complimenting the "alpha sarcin" binding site, as for T. thermophilus. Bases 2646–2667 (E. coli's equivalents)

Table VIII. DNA oligommeres, complementary to exposed rRNA o, crystallizable ribosomal particles

Probing exposed rRNA by complementary DNA oligomers gained recently considerable popularity for mapping the ribosome surface. It was found that AUG and dATG containing oligomers promoted the non-enzymatic binding of fmet-tRNA with similar properties and formed initiation complexes which are fully reactive with puromycin. In parallel, for illuminating the formation of the initiation complex, the competition between a variety of cDNA oligomers and poly(U), poly(AUG), tRNAphe, tRNAfmet and the initiation factors were monitored. In addition, anti-sense DNA was proved instrumental in monitoring dispositions of normal and altered *E. coli* 16S rRNA (26).

Exposed single-stranded rRNA segments which may be complemented by

Accessible primary amino groups were probed by methylation or acylation, following the procedures used for a muscle protein (32) and lysozyme (33). As expected, onlyin a few occasions the methylation of the ribosomal particles reached completeness. Hence only partial information about the surface of the ribosomes could so far be obtained. In typical experiments 25–60% of the lysines of H50S became methylated. Interestingly, the H50S particles which were exposed to lower methylation levels (25% of the original amount) yielded crystals, which on several occasions reached an unusual large size (26). The small halophilic ribosomal subunits behave differently. Upon methylation under the original conditions as well as by milder ones, substantial disintegration was observed. These observations accord well with the lower stability and higher sensitivity found for several small eubacterial ribosomal subunits by different methods (6,34–35). In contrast, T30S was readily methylated to completion while maintaining its integrity. In these experiments 70% of its lysines became methylated, indicating that the rest 30% of the lysines are engaged in internal contacts, presumably with the ribosomal RNA.

A halophilic rRNA-protein complex. To assist the interpretation of the anticipated electron density map, a specific internal rRNA-protein complex of protein HmaL1 and a stretch of H23S rRNA was isolated from the halophilic ribosome (36). Although it remains to be seen whether the structures of the crystallized isolated r-proteins do reflect their in-situ conformations, their mere crystallization may indicate the existence of intrinsic fold. For three decades extensive efforts have been made in several laboratories to crystallize isolated ribosomal components. These include whole or fragmented RNA chains as well as isolated proteins and their clusters (37). So far experience showed that in general assembled ribosomal particles crystallize more readily than most of their isolated components. In fact, the majority of the r-proteins could not crystallize, and as of yet, the structures of most of the crystallized components have not been solved, mainly due to the poor internal order of their crystals. This rather low yield indicates that the conformations of many ribosomal components are dictated by their environment, namely by the network of internal contacts which construct the skeleton of the ribosome. Thus, those proteins that do not possess an independent intrinsic conformation may loose their in situ conformation when detached from the scaffolding ribosomal network. Protein BL11 is an example of a ribosomal protein which undergoes significant, albeit reversible, conformational changes upon isolation from the 50S subunit. On the ribosome its -SH group is exposed and reactive, whereas in solution this group is buried and becomes reactive only under denaturing conditions (6 M urea). However, the lost native conformation of the isolated protein is regained upon its reconstitution into core particles, even when large chemical moieties are bound to its - SH group (19).

The higher suitability of the thermophilic isolated r-proteins for crystallographic studies over those from *E. coli* shows that under proper conditions some isolated ribosomal components can be trapped in a unique conformation. Encouraged by these findings, we focused our efforts on the purification and the crystallization of isolated components from halophilic ribosomes, which are supposed to be more robust. Furthermore, internal defined ribonucleoprotein complexes, should be more suiTable for crystallographic studies than isolated proteins or rRNA fragments, as they are more likely to maintain the native conformation since within such complexes the micro environment may be partially kept. The complex of protein HmaL1 and a segment of H23S rRNA was isolated by decreasing the salt concentration below the minimum needed for preserving the structure of the entire 50S subunit. In these experiments it was clearly shown that among the 23S RNA binding proteins, protein HmaL1 has the highest specific affinity, sufficient to remain bound in quantitative amounts to the 23S rRNA throughout the extraction procedure (36).

Ribosomes were found to be highly conserved throughout evolution. Numerous phylogenetic studies were based on the comparative analysis of individual ribosomal components. Thus, it was found that protein EL1 recognizes defined binding sites on 23S rRNA and 26S RNA chains from various organisms of the three kingdoms (eubacteria, archaebacteria and eucaryotes) and forms specific heterologousribonucleoprotein complexes with those chains (38). Similarly, chimeric complexes were reconstituted between the components of the halophilic complex and the corresponding *E. coli* ribosomal components, indicating a rather high homology, despite the evolution distance and the substantial differences in the physiological environment and standard binding conditions for the ribosomes of these two bacteria.

Approximating the shapes of the ribosomal particles using crystalline monolayers

Images of the ribosome and its large subunit were reconstructed from tilt series of crystalline arrays, negatively stained with an inert material, goldthioglucose (15–16). Although the image reconstruction procedure is not free from experimental and conceptual limitations, its superiority over conventional electron microscopy methods was demonstrated by the conclusive and exclusive detection of several key features, associated mainly with internal vacant or partially filled hollows. Thus, the ribosome, which until recently was believed to be a compact particle, is currently conceptualized as a rather porous organelle, containing holes, cavities, tunnels, gaps and voids, some of which could be tentatively interpreted.

A plausible interpretations of the low resolution reconstruced models

Despite their rather low resolution (47 and 28 Å, for 70S and 50S particles, respectively) and the other shortcomings inherent to electron-microscopy studies, the models of the ribosomal particles provided a valuable aid for further studies. The significant similarities in corresponding regions in the reconstructed models of the 50S and 70S particles were exploited for assessing their reliability, for suggesting a possible location of the 50S subunit within the 70S ribosome, for providing a plausible description of the conformational changes which may accompany the association of the ribosomal subunits, for extracting an approximate model for the bound 30S subunit and for tentative assignments of biological functions to several structural features, described below (6,8,30,34, 39–40).

A tunnel in large ribosomal subunit may provide a protected path for nascent proteins.

A few elongated features of low density were clearly observed in the models reconstructed for the large subunit and the whole ribosome. One of these tunnels (t1 in Figure 4) is about 100–120 è in length and up to 25 Å in diameter (15,34,39–40), dimensions similar to those observed in the reconstruction from crystalline arrays of 50S subunits from *T. thermophilus* (Y. Fujiyoshi, personal communication). A feature, similar to this tunnel was also detected within the density map obtained at 30 Å resolution from neutron diffraction data, collected from three-dimensional crystals of 50S subunits from *H. marismortui* (5). It is noteworthy that in 1983, a hole was detected within the 50S subunit obtained by the optimized series expansion reconstruction method (41). In addition, a channel was seen in images reconstructed at 50–60 resolution, of eukaryotic 80S ribosomes from chick-embryos (42). Furthermore, two internal holes with no obvious functional roles were detected in the random-conical reconstructed models of single 50S subunits and 70S ribosomes from *E. coli* (43–44). Visual examination indicated that at a proper contour level, these holes may be connected to form a comparable tunnel. Interestingly, at this contour level the length of the extended arm (assigned as L7/12) is somewhat shorter than in the conventional consensus models, closer to that observed for particles embedded in amorphous ice or by reconstruction from crystalline arrays (37). Evidence derived from biochemical, fluorescence and functional experiments, obtained first in the sixties and reconfirmed recently, indicate that ribosomes mask the latest synthesized part of newly formed proteins (35,45–54). Complementary information was obtained by immuno-electron-microscopy, showing that nascent proteins emerge out of the 50S subunit, opposite to the site of the formation of the peptide bond, the peptidyl transferase center (55). It is note-

worthy that large variations in the number of protected residues have emerged from different biochemical experiments. Some indicated as little as 25 protected residues, whereas in others, only chains which reached the length of 70–130 amino acids became exposed to a large variety of compounds, ranging from small, such as iodine, to very large ones, such as IgG (52) or DnaJ and DnaK molecules (54).

It was found that the various reconstructed models of the crystalline 50S subunits are almost indistinguishable (6,30,40), whereas those derived from crystalline 70S ribosome differ in bulkiness, but are of comparable dimensions and share common prominent features (30–40). The positioning of the 50S subunit within the 70S ribosome (Figure 4) was based solely on objective structural arguments, namely, on the similarities in specific features observed in the reconstructed models. Thus, the 50S subunit was placed within the 70S ribosome in an orientation which allows best fit between the external shapes of the two particles, while the direction of the main tunnel in the 50S subunit matches that of tunnel t1 in the 70S ribosome (Figure 4). Differences were detected in the shapes of free 50S subunits, and those assigned as it in the associated 70S ribosome (34,40). These may result from the resolution limits at which the two images were reconstructed (28 vs. 47 Å), but also may reflect real conformational changes occurring upon the association of the two ribosomal subunits to form the 70S ribosome.

A groove in the 30S subunit was suggested as the mRNA path.

A distinct region of crowded rRNA was revealed within the part of the reconstructed 70S ribosome which was assigned as the 30S subunit (39,39–40). A similar region of high stain-density was detected by electron microscopical investigations of isolated 30S subunits (56). In accord with cross-linking and model-building experiments indicating that the mRNA binds to the 30S subunits in an environment rich in rRNA (57–59), and with biochemical evidence showing that during translation a segment of about 30–40 nucleotides of mRNA is masked by the ribosome (60), this groove was tentatively identified as the mRNA progression path. The resolution of the current reconstructed images is too low for an accurate determination of the dimensions of the groove, but a rough estimate indicates that it may accommodate a stretch of mRNA in random, U-shaped or helical conformations with a length comparable to that found to be masked by the ribosome.

The intersubunit free space was assigned as the site of protein biosynthesis.

A free space of about 20% of the total volume, was first detected in models reconstructed from crystalline 70S ribosomes from *B. stearothermophilus* (Figure 2 and ref. 16). This free space was interpreted as the separation between

the small and the large subunits. Similar intersubunit-gaps of varying sizes were observed in almost all the so far reported reconstructions of whole ribosomes, regardless of the reconstruction method, the source of the ribosomes and the level of organization: single particles (44,61), in situ sheets (42), in vitro grown two-dimensional crystalline arrays (16,34) and *in vivo* normal and starved particles (62). Additional support for a sizable free space at the intersubunit interface was provided by phylogenetic studies, which showed no evidence for direct base pairing between the two subunits (63). Interestingly, even the tight intersubunit rRNA clustering, suggested from crosslinking and fingerprinting studies, could be accommodated, after slight rearrangements, in the limited area which can be available for direct contacts between the two ribosomal subunits at the interface around the void (64).

The functional assignments described above led to the suggestion that the intersubunit free space is the location where the various enzymatic activities, involved in protein biosynthesis, occur. The shape and the dimensions of tRNA allow its placement in the intersubunit space, so that its anticodon loop may associate with the mRNA, and its CCA-terminus is positioned so that the newly formed peptidyl group can extend into the entrance to the tunnels. In this orientation the tRNA molecule may also form several non-cognate interactions with the walls of the free space (Figure 5). At the current resolution of the reconstructions, the two crystallographically determined orientations of tRNA: the native-closed and the bound-open one (65) are practically indistinguishable. The positioning of the tRNA molecules within the intersubunit space accords well with a large volume of circumstantial evidence accumulated during the last two decades 30,66). It is further supported by recent findings which show that upon binding to 70S ribosomes, the entire P-site tRNA molecule is inaccessible even to hydroxyl radicals (67).

Although no more than two tRNA molecules are bound to the ribosome simultaneously, three different tRNA binding sites were proposed (68). Indeed, steric considerations showed that the intersubunit void is spacious enough to provide up to three tRNA binding sites, alongside with the space needed for the other non-ribosomal components participating in protein biosynthesis. It is noteworthy that the intersubunit space allows the location of the tRNA molecules in various relative orientations, ranging from parallel, the lowest space-requiring arrangement, to perpendicular (Figure 5), the highest space-consuming one (66).

The advancing nascent peptide.

A large volume of experiments have been designed for analyzing the sequences, conformations and maximum lengths of the growing protein chains, which can be accommodated in the tunnel. The progression of growing peptides was followed by several techniques (69). Of particular interest are the studies about

the fate of the MS2 coat protein. This is an optimal candidate for studying the progression of nascent chains, not only because of the availability of its mRNA, but also because in its native conformation its N-terminal methionine (70) is pointing outward (71). It was found that a coumarin at the N-terminus of the nascent MS2 peptide was shielded from interacting with its IgG until the protein reached its full length, 129 amino acid residues.

The crystallographically determined structure of MS2, which is a nearly spherical protein of a relatively compact structure, composed of seven antiparallel beta-strands and two short alpha-helices (71) and the reconstructed models of the ribosomal particles were the basis for modelling experiments (69).

The C-terminus of the MS2 protein was placed in the vicinity of the suggested peptidyl transferase center, and the main chain along the tunnel in a partially unfolded conformation, while maintaining the native fold of long stretches of the beta-structures as well as the native conformation of the segment 1–47, which reached the exit of the tunnel (Figure 6). These modelling efforts showed that a chain of 129 residues can be accommodated within the tunnel in a partially folded beta-sheets conformation. Furthermore, the graphic representation validates the suggestion derived from immuno-fluorescence experiments, that the progressing N-terminus may be partially or fully folded (69,72), as well as of activation-release studies, showing that the final steps in the folding of nascent proteins are mediated by chaperons associating with the ribosome (73).

Does the growth of homopolypeptides mimic that of proteins?

For over three decades the universal procedure for determining the extent of functional activity of ribosomes was based on programming them with poly(U) or poly(A) and monitoring the production of polyphenylalanine or polylysine, respectively. For this purpose this procedure is informative, efficient and reproducible. Nevertheless, new compelling evidence indicated that these two homopolypeptides are rather poor candidates for the accurate and quantitative analysis of the structural properties of nascent proteins, due to the nature of the measurements and to the inherent differences between the chemical properties of homo- and hetero-polypeptides. Thus, striking differences were observed in the progression of nascent proteins and those of polyphenylalanine and polylysine. The uniqueness of the path utilized by polyphenylalanine was firmly established (52,83) and it was concluded that in contrast to naturally occurring proteins, polyphenylalanine is formed as an insoluble mass located initially in the vicinity of the peptidyl transferase center (74).

In experiments aimed at the verification of the existence of an internal path for nascent polypeptide, N-termini of nascent homo-polypeptides were detected by immuno-electron-microscopy at two distinct patches on the 50S subunit. Short

polypeptides were observed close to the subunit interface, whereas longer ones at the far end of this particle (48). It is conceivable that a specific common feature, located at the amino termini of natural proteins has a role in guiding them into the tunnel. It is still unclear whether this feature should bear a special structural motif, a chemical affinity to the entrance of the tunnel, or both. A few suggestions have been made, mostly associated with the occurrence of methionines and formyl-methionine at the N-terminus of native proteins, as well as with specific chemical affinities and/or electrostatic properties, but none led to a conclusive hypothesis.

A failure of a nascent peptide in entering the tunnel may be fed back into the biosynthetic machinery at early stages and lead to premature termination of the process. This hypothesis may explain the inhibition of peptide synthesis by erythromycin. It also sheds light on the discrepancy between the rather small fraction (around 50%) of well prepared ribosomes found to be active in in vitro production of relatively long polypeptides, and the almost quantitative binding of mRNA and tRNA of similar preparations (10,75). In addition, it may shed light on the differences observed in the migration of short and long chains of newly synthesized polylysine or polyphenylalanine.

It was found that under appropriate experimental conditions, newly formed polyphenylalanine and polylysine may adhere to the large ribosomal subunits of *E. coli* (76), *B. stearothermophilus* (77,39) and *H. marismortui*, (15,39), even after the interruption of the biosynthetic process and dissociation of the ribosome. This attachment is tight enough to allow co-crystallization of short nascent homopolypeptides with 50S subunits. Thus, it seems that the exit path of these nascent homopolypeptides is composed of rRNA and hydrophobic patches, the components which are most likely to interact with polylysine and polyphenylalanine, respectively. It is noteworthy that the rigidity introduced to proline-rich chains, presumably by the very nature of the proline ring, was found to slow their progression (35). This finding is in accord with the fold suggested for segments of globular proteins rich in prolines. Thus, an extended rather stiff conformation was postulated for the sequence $(pro\text{-}x)_4$ in sorbitol dehydrogenase (78).

Crystallizable ribosomal complexes mimicking defined functional states

The image-reconstruction studies, mentioned above, stimulated the design and the crystallization of complexes of ribosomal particles, mimicking defined functional states in the process of protein biosynthesis (Table III and refs. 10,77). Unfortunately the crystals of the complexes of 50S subunits with short nascent homopolypeptides are still too small for crystallographic data collection. How-

ever, more exciting results have been obtained from the complexes of the whole 70S ribosome. All three-dimensional crystals of 70S particles obtained so far, namely from *E. coli*, *B. stearothermophilus* and *T. thermophilus*, are either too small or diffract to a very low resolution, 20–45 Å (79–81). This property was attributed to the inherent flexibility of the ribosome, which could be made possible by its large intersubunit void, as it may provide the mobility needed for the process of protein biosynthesis. This intrinsic flexibility may result in significant conformational heterogeneity. In fact, it is believed that each preparation of 70S ribosomes is comprised of particles at several conformations. Some ribosomes aretrapped in defined states of the tranlational cycle, whereas others, devoid of some of the non-ribosomal biosynthetic components, may assume high flexibility.

To minimize the flexibility and to increase the homogeneity of the crystallized material, complexes were prepared, containing ribosomes trapped in conformations mimicking defined stages in protein biosynthesis. A simple complex, composed of 70S ribosome from *T. thermophilus* with two phetRNA^{phe} molecules and a chain of about 35 uridyl residues, was crystallized. In this complex the mRNA is of a length which may fit in the groove found in the 30S subunit so that no long stretches of it project out, the intersubunit space is rather full, and most of the ribosomes are "trapped" in a similar conformation.

Despite the non optimal composition of this complex, which allows substantial freedom in the binding of the mRNA (polyU), a dramatic improvements in the reproducibility of crystal growth and in the internal order of the crystals were observed. Whereas the best three-dimensional crystals of 70S ribosomes diffract to 20–24 Å resolution (80–81), those grown from this complex exhibit sharp diffraction patterns to 12-14 Å (10). To assess the individual contributions of the different components to the stability of this complex, 70S ribosomes were cocrystallized with a chain of 35 uridines. Only poorly shaped three-dimensional crystals were occasionally obtained, indicating the larger contribution of the tRNA to the stability of the complex. Since tRNA participates in all crystallized complexes of ribosomal particles, trapped at defined functional states (Table IX), the undecagold cluster was attached to it, in a fashion which does not impair its amino-acylation and allows its binding to ribosomes (10). This type of specific derivatization should not only lead to phasing but also illuminate one of the most interesting aspects of protein synthesis: the modes of binding of the tRNA molecules to the ribosome.

Although the present finding led to better understanding of the ribosomal structure, it is clear that a higher resolution is essential for more accurate assignments. Therefore image reconstructions experiments from unstained crystalline arrays in vitrified ice are being carried out. Preliminary efforts led to the growth of arrays of 50S subunits, diffracting to about 15 Å resolution (82).

ever, more exciting results have been obtained from the complexes of the whole 70S ribosome. All three-dimensional crystals of 70S particles obtained so far, namely from *E. coli*, *B. stearothermophilus* and *T. thermophilus*, are either too small or diffract to a very low resolution, 20–45 Å (79–81). This property was attributed to the inherent flexibility of the ribosome, which could be made possible by its large intersubunit void, as it may provide the mobility needed for the process of protein biosynthesis. This intrinsic flexibility may result in significant conformational heterogeneity. In fact, it is believed that each preparation of 70S ribosomes is comprised of particles at several conformations. Some ribosomes aretrapped in defined states of the tranlational cycle, whereas others, devoid of some of the non-ribosomal biosynthetic components, may assume high flexibility.

To minimize the flexibility and to increase the homogeneity of the crystallized material, complexes were prepared, containing ribosomes trapped in conformations mimicking defined stages in protein biosynthesis. A simple complex, composed of 70S ribosome from *T. thermophilus* with two phetRNA^{phe} molecules and a chain of about 35 uridyl residues, was crystallized. In this complex the mRNA is of a length which may fit in the groove found in the 30S subunit so that no long stretches of it project out, the intersubunit space is rather full, and most of the ribosomes are "trapped" in a similar conformation.

Despite the non optimal composition of this complex, which allows substantial freedom in the binding of the mRNA (polyU), a dramatic improvements in the reproducibility of crystal growth and in the internal order of the crystals were observed. Whereas the best three-dimensional crystals of 70S ribosomes diffract to 20–24 Å resolution (80–81), those grown from this complex exhibit sharp diffraction patterns to 12-14 Å (10). To assess the individual contributions of the different components to the stability of this complex, 70S ribosomes were cocrystallized with a chain of 35 uridines. Only poorly shaped three-dimensional crystals were occasionally obtained, indicating the larger contribution of the tRNA to the stability of the complex. Since tRNA participates in all crystallized complexes of ribosomal particles, trapped at defined functional states (Table IX), the undecagold cluster was attached to it, in a fashion which does not impair its amino-acylation and allows its binding to ribosomes (10). This type of specific derivatization should not only lead to phasing but also illuminate one of the most interesting aspects of protein synthesis: the modes of binding of the tRNA molecules to the ribosome.

Although the present finding led to better understanding of the ribosomal structure, it is clear that a higher resolution is essential for more accurate assignments. Therefore image reconstructions experiments from unstained crystalline arrays in vitrified ice are being carried out. Preliminary efforts led to the growth of arrays of 50S subunits, diffracting to about 15 Å resolution (82).

70S Ribosomes + poly(U) (30–35 mers) + 2 phe-tRNAphe
70S Ribosomes + poly(U) (30–35 mers)
50S subunits + $tRNA^{phe}$ + poly phenylalanine (10–18 mers)
50S subunits + $tRNA^{lys}$ + poly lysine (10–18 mers)

Table IX. Crystallized functional complexes.

Conclusions and prospects

We have demonstrated that crystallographic studies on intact, modified, complexed and mutated ribosomal particles are well underway. From the early stages of this work, it has been clear that a straight-forward application of conventional concepts and techniques of macromolecular crystallography would not be adequate. Our approach combines the exploitation of the extensive information available on the genetic, functional and chemical properties of ribosomes for a rational design of protocols for crystallization and for derivatization with dense clusters or multi-atom salts.

However, the way for structure determination is yet far from being paved, and significant innovation and sophistication are essential for each of the stages of the crystallographic studies. Furthermore, the complexity, sensitivity to external conditions and the inherent conformational flexibility of all ribosomal particles, including those believed to be rather robust ones, hamper most of the supportive non- crystallographic experiments. Nevertheless, valuable information has already been obtained, and is being exploited in the design of our further experiments.

Acknowledgements

The studies presented here have been initiated under the inspiration and guidance of the late Prof. H.G. Wittmann. We would like to thank Drs. M. Pope and F. Triana for their gifts of multi-atom salts and tRNA molecules, respectively. We also thanks Drs. M. Roth, E. Pebay-Peyroula, B. Hardesty, T. Choli, A. Podjarny, W. Hill, E. Dabbs, K.R. Leonard and W. Chiu for their active participation in the studiespresented here and for their illuminating comments.

This work was carried out at the Weizmann Institute of Science, the Max-Planck-Research-Unit at DESY in Hamburg, the Max-Planck-Institute for Molecular Genetics in Berlin, and at the following synchrotron facilities: EMBL and MPG beam lines at DESY, Hamburg; CHESS, Cornell University; SSRL, Stanford University; and PF/KEK, Japan.

Support was provided by the National Institute of Health (NIH GM 34360), the German Federal Ministry for Research and technology (BMFT 05 180 MP BO) and the national science foundation, DFG (Yo-11/1-2), The German space agency DARA (50QV 86061), the Minerva Fellowship Program, and the Kimmelman Center for Macromolecular Assembly at the Weizmann Institute. AY holds the Martin S. Kimmel Professorial Chair.

References

1. Maaloe O. In "Biological regulation and development" (Goldstein R.F., ed.) Vol 1, Plenum Publ. C. N.Y. 1979, 487
2. Noller HF, Hoffarth V and Zimniak L. Science 1992, 256, 1416
3. Picking WD, Odom OW and Hardesty B. Biochemistry 1992, 31, 12565
4. von Boehlen K, MakowskiI, HansenHAS, Bartles H, Berkovitch-Yellin Z, Zaytzev-Bashan A, Meyer S, Paulke C, Franceschi F and Yonath A. J. Mol. Biol. 1991, 222,11.
5. Eisenstein M., Sharon R., Berkovitch-Yellin Z., Gewitz H.S., Weinstein S., Pebay-Peyroula E., Roth M. and Yonath A. (1991) Biochemie, 73, 879
6. Berkovitch-Yellin Z., Bennett W.S. and Yonath A. (1992) CRC Rev. Biochem. & Mol. Biol. 27:403-444
7. Berkovitch-Yellin Z., Hansen H.A.S., Weinstein S., Eisenstein M., von Bîhlen K., Agmon I., Evers U., Thygesen J., Volkmann N., Bartels H., Schlânzen F., Zaytzev-Bashan A., Sharon R., Levin I., Dribin A., Kryger G., Bennett W.S., Franceschi F. and Yonath A. in: "Synchrotron Radiation & Mol. Biol.", (B. Chance et al., eds.) Clarendon Press (1994) 61
8. Franceschi F., Weinstein S., Evers U., Arndt E., Jahn W., Hansen H.A.S., von Boehlen K., Berkovitch-Yellin Z., Eisenstein M., Agmon I., Thygesen J., Volkmann N., Bartels H., SchlÅnzen F., Zaytzev- Bashan A., Sharon R., Levin I., Dribin A., Sagi I., Choli- Papadopoulou T., Tsiboly P., Kryger G., Bennett W.S. and Yonath A. (1993) In Nierhaus et al., 391
9. Hope, H., Frolow, F., von Bîhlen, K., Makowski, I., Kratky, C., Halfon, Y., Danz, H., Webster, P., Bartels, K., Wittmann, H.G. and Yonath, A., (1989) Acta Cryst., B45, 190
10. Hansen H., Volkmann N., Piefke J., Glotz C., Weinstein S., Makowski I., Meyer S., Wittmann H.G., Yonath A., (1990) Biochem. Biophys. Acta, 1050,1
11. Bricogne, G., (1991) Acta Cryst. A47, 803
12. Gilmore, C.J., Henderson, G., Bannister, C. (1990), Acta Cryst. A47, 830
13. Carter, C.W., Crumley, K.V., Coleman, D.E., Hage, F. and Bricogne, G. (1990) Acta Cryst. A46, 57
14. Roth M., Lewit-Bentley A., Michel H., Deisenhofer J., Huber R. & Oesterheld D., (1989) Nature 340, 659
15. Yonath A., Leonard K.R. and Wittmann H.G. (1987) Science 236, 813
16. Arad T., Piefke J., Weinstein S., Gewitz H.S., Yonath A., Wittmann H.G. (1987) Biochimie 69, 1001
17. Jahn, W., (1989a) Z. Naturforsch., 44b, 1313

18. Jahn, W., (1989b) Z. Naturforsch., 44b, 79
19. Weinstein S., Jahn W., Hansen H.A.S., Wittmann H.G. and Yonath A. (1989) J. Biol. Chem. 264, 19138
20. Weinstein S., Jahn W., Laschever M., Arad T., Tichelaar W., Haider M., Glotz C., Boeckh T., Berkovitch-Yellin Z., Franceschi F. and Yonath A. (1992) J. Crystal growth, 122, 286
21. Harms, J. SchlÅnzen F., von Bîhlen K., Thygesen J., Meyer S., Dunkel I., Donzelmann B., Hansen H.A.S., Zaytzev-Bashan A., Dribin A., Kryger G., Thoms G., Volkmann N., Bartels H., Bennett W.S. & Yonath A. (May 1993) ESF Report 26
22. Schnier J., Gewitz H.S. Behrens E., Lee A., Ginther G. and Leighton T. (1990) J. Bacteriol., 172, 7306
23. Gewitz H.S., Glotz C., Goischke P., Romberg B., MÅssig J., Yonath A. and Wittmann H.G. (1987) Biochem. Intern. 15, 887
24. Amils R., Ramirez L., Sanz J.L., Martin I., Pisabarro A.G., E. Sanchez and D. Urena. In Hill et al., (1990) 645
25. Franceschi F., Sagi I., Bîddeker N., Evers U., Arndt E., Paulke C., Hasenbank R., Laschever M., Glotz C., Piefke J., MÅssig J., Weinstein S., and Yonath A. (994) Syst. & App. Microbiology, 16, 697
26. Sagi I., Weinrich W., Levin I., Glotz C., Laschever M., Melamud M., Franceschi F., Weinstein S. and Yonath A., Biophys. J. 1995, in the press.
27. Arndt E. and Weigel C. (1990) Nucleic Acid Res. 18, 1285
28. Arndt E. and Steffens C. (1992) FEBS Lett. 314,211
29. Kruft V. and Wittmann-Liebold B. (1991) Biochemistry, 30, 11781
30. Yonath A. and Berkovitch-Yellin Z. (1993) Current Opinion in Structural Biology, 3, 175
31. Weller J. and Hill W.E., Biochemie (1991) 73, 971
32. Rayment I., Rypniewski W.R., Schmidt-Baese K., Smith R., Tomchick D.R., Benning M.M., Winkelmann D. A., Wesenberg G., and Holden H.M. (1993) Science 261, 50
33. Rypniewski W.R., Holden H.M., Rayment I., Biochemistry, (1993) 32, 9851
34. Yonath A. and Wittmann H.G. (1989) TIBS 14, 329
35. Evers U., Gewitz H.S. (1989) Biochem. Internat 19, 1031
36. Evers U., F. Franceschi, N. Boeddeker and A. Yonath (1994) Bioph. Chem. 50, 3
37. Yonath A. and Franceschi F. (1993) Current Opinion in Structural Biology, 3, 45
38. Zimmermann R.A., Thurlow D.L., Finn R.S., Marsh T.L. and Ferrett L.K. (1980) in RNA Polymerases, tRNA and Ribosomes: Their Genetics and Evolution (Osawa, S., Ozeki, H., Uchida, H. and Yura, T., eds) (1980), Univ. of Tokyo Press, Tokyo, 599
39. Yonath A., Bennett W.S., Weinstein W. and Wittmann H.G. In Hill et al., (1990) 134
40. Berkovitch-Yellin Z., Wittmann H.G., Yonath A. (1990) Acta. Cryst. B46, 37
42. Milligan R.A., Unwin P.N.T. (1986) Nature 319, 693
43. Radermacher M., Srivastava S. and Frank J. (1992) Abs 19, European EM Conference, Granada.

44. Frank J., Penczek P., Grassucci R. and Srivastava S. (1991) J. Cell. Biol., 115, 597
44. Smith W.P., Tai P.C. and Davis B.D. (1978) Proc. Natl. Acad. Sci. USA. 75, 5922
45. Malkin L.I. and Rich A. (1967) J. Mol. Biol. 26, 329
46. Blobel G., Sabatini D.D. (1970) J. Cell. Biol. 45, 130 von Boehlen K., Makowski I., Hansen H. A. S., Bartels H., Berkovitch-Yellin Z., Zaytzev-Bashan A., Meyer S., Paulke C., Franceschi F. and Yonath, A. (1991) J. Mol. Biol., 222, 11
48. Ryabova L.A., Selivanova O.M., Baranov V.I., Vasiliev V.D., Spirin A.S. (1988) FEBS Lett. 226, 255
49. Yen I.J., Macklin P.S. and Cleavland D.W. (1988) Nature 334, 580
50. Kurzchalia S.V., Wiedmann M., Breter H., Zimmermann W., Bauschke E., Rapoport T.A. (1988), European J. of Biochem., 172, 663
51. Kolb V.A., Kommer A., Spirin A.S. (1990) Workshop on Translation, Leiden, p.84a.
52. Hardesty B., Odom O.W., Kudlicki W. and Kramer G. (1993) In K. Nierhaus, et al., 347
53. Crowley, K.S., Reinhart, G.D. and Johnson A.E. (1993) Cell, 73, 1101
54. Hartl F.U. Abs. 19, (1993) EMBL Conference on Structural Biology, Heidelberg Hill W.E., Dahlberg A., Garrett R.A., Moore P.B., Schlesinger D. and Warner J.R. (Eds.) "The Ribosome: Structure, Function and Evolution", ASM Publications, Washington, USA (1990)
55. Bernabeu C., Lake J.A. (1982) Proc. Natl. Acad. Sci., USA. 79, 3111
56. Oakes M., Scheiman A., Atha T., Shakweiler G., Lake J. In Hill et al.(1990), 180
57. Brimacombe, R., Atmadja, J., Stiege, W. and Schueler, D., (1988) J. Mol. Biol., 199, 115
58. Brimacombe R., Greuer B., Mitchell P., Osswald M., Rinke-Appel J., Schueler, D., Stade K. (1990) In Hill etal., (1990) 93
59. Rinke-Appel J., Junke N., Stade K. and Brimacombe R. (1991) The Path of mRNA Trough the E. Coli Ribosome; Site Directed Cross-Linking of mRNA Analogues Carrying a Photo-Reactive Label at Various Points 3' to the Decoding Site. EMBO J. 10, 2195
60. Kang C. and Cantor C.R. (1985) J. Mol. Biol. 210, 659
61. Wagenknecht T., Graassucc R. and Frank J. (1989) J. Mol. Biol. 199, 137
62. Ofverstedt L.G., Zhang K., Tapio S, Skuglund U. and Isaksson L., (1994) Cell, 79, 629
63. Larsen N. (1992) Proc. Nat. Acad. Sci. USA 89, 5044
64. Mitchell P., Osswald M. and Brimacombe R. (1992) Biochemistry, 31, 3004
65. Moras D. (1989) Landolt-Borstein New Series 1b. Nucleic Acids. (W Seanger ed.) Spreinger Verlag. Berlin Heidelberg & NY. 1
66. Spirin A. (1987) Biochemie, 69, 949
67. Huettenhofer A. and Noller H.F. (1992) Proc. Nat. Acad. Sci., 89, 7851
68. Nierhaus K.H., Franceschi F., Subramanian A.R., Erdmann V. and Wittmann-Liebold B. (Eds): "The translational Apparatus". Plenum Publishing Corp. New York, (1993)
69. Eisenstein M., Hardesty B., Odom M., Kudlicki W., Kramer G., Arad T., Franceschi F. & Yonath A. (1994) In: Supramolecular Structure (G. Pifat Ed.) Balaban Press, Rehovot, 213
70. Jau W.M., Haegeman G., Ysebaert M. and Fiers W. Nature 1972, 237, 82

71. Valegard K., Liljas L., Friborg K. and Unge T. (1990) Nature, 345, 36
72. Hardesty B., Yonath A., Kramer G., Odom O.W., Eisenstein M., Franceschi F. and Kudlicki W. In: Membrane Protein Transportp (S.S. Rothman, Ed.), in the press (1995)
73. Kudlicki W., Odom O.W., Kramer G. and Hardesty B. (1994) In J. Biol. Chem.
74. Odom O.W., Picking W.D., Tsalkova T. and Hardesty B. (1991) Eur. J. Biochem. 198, 713
75. Rheinberger H.J. and Nierhaus K.H. (1992) Europ. J. of Biochem. 193, 643
76. Gilbert W. (1963) Cold Spring Harbor Symposium on Quantitative Biology 28, 287
77. Gewitz H.S., Glotz C., Piefke J., Yonath A. and Wittmann H.G. (1988) Biochimie, 70, 645
78. Eklund H., Horjales E., Jornvall H., Branden C.-I., Jeffery J. (1985) Biochemistry, 24, 8005
79. Wittmann H.G., Muessig J., Gewitz H.S., Piefke J., Rheinberger H.J. and Yonath A. (1982) FEBS Letters 146, 217
80. Trackhanov S.D., Yusupov M.M., Shirokov V.A., Garber M.B., Mitschler A., Ruff M., Thierry J.C. and Moras D. (1989) J. Mol. Biol. 209, 327
81. Berkovitch-Yellin Z., Hansen H., Bennett W.S., Sharon R., von Boehlen K., Volkmann N., Piefke J., Yonath A., Wittmann H.G. (1991) J. Crystal Growth, 110, 208
82. Avila-Sakar A.J., Guan T.L., Schmid M.F., Loke T.L., Arad T., Yonath A., Piefke J., Franceschi F. and Chiu W. (1994), J. Mol. Biol.,239, 689
83. Picking W.D., Odom O.W., Tsalkova T., Sordyu K.T. and Hardesty B. (1991) J. Biol. Chem. 266, 1534